Received: 7 March 2017 | Accepted: 14 August 2017

DOI: 10.1111/gcb.13886

PRIMARY RESEARCH ARTICLE

WILEY Global Change Biology

Detection of climate change-driven trends in phytoplankton phenology

Stephanie A. Henson[1] | Harriet S. Cole[2] | Jason Hopkins[3] | Adrian P. Martin[1] | Andrew Yool[1]

[1]National Oceanography Centre, Southampton, UK

[2]Marine Scotland, Marine Laboratory, Aberdeen, UK

[3]Bigelow Laboratory for Ocean Sciences, East Boothbay, ME, USA

Correspondence
Stephanie A. Henson, National Oceanography Centre, Southampton, UK.
Email: s.henson@noc.ac.uk

Funding information
Seventh Framework Programme, Grant/Award Number: 264933; Natural Environment Research Council, Grant/Award Number: NE/H017372/1

Abstract

The timing of the annual phytoplankton spring bloom is likely to be altered in response to climate change. Quantifying that response has, however, been limited by the typically coarse temporal resolution (monthly) of global climate models. Here, we use higher resolution model output (maximum 5 days) to investigate how phytoplankton bloom timing changes in response to projected 21st century climate change, and how the temporal resolution of data influences the detection of long-term trends. We find that bloom timing generally shifts later at mid-latitudes and earlier at high and low latitudes by ~5 days per decade to 2100. The spatial patterns of bloom timing are similar in both low (monthly) and high (5 day) resolution data, although initiation dates are later at low resolution. The magnitude of the trends in bloom timing from 2006 to 2100 is very similar at high and low resolution, with the result that the number of years of data needed to detect a trend in phytoplankton phenology is relatively insensitive to data temporal resolution. We also investigate the influence of spatial scales on bloom timing and find that trends are generally more rapidly detectable after spatial averaging of data. Our results suggest that, if pinpointing the start date of the spring bloom is the priority, the highest possible temporal resolution data should be used. However, if the priority is detecting long-term trends in bloom timing, data at a temporal resolution of 20 days are likely to be sufficient. Furthermore, our results suggest that data sources which allow for spatial averaging will promote more rapid trend detection.

KEYWORDS
bloom initiation, bloom timing, climate model, climate warming, ocean monitoring, RCP8.5, sustained observations

1 | INTRODUCTION

Phenology refers to the characteristics of naturally recurring events, such as the seasonal cycles of plants and animals. Phenology has been recognised by the Intergovernmental Panel on Climate Change (IPCC) as 'perhaps the simplest process in which to track changes . . . in response to climate change' (Rosenzweig et al., 2007). In the ocean, the seasonal cycle of primary production is dominated in many regions by the annual phytoplankton spring bloom (Gran & Braarud, 1935). In a meta-analysis of recorded climate change impacts on marine species, Poloczanska et al. (2016) found that phytoplankton phenology was almost exclusively shifting earlier in the year. Long time series of data (>30 years) are expected to be necessary to distinguish a climate change-driven trend in phytoplankton

populations from natural variability (Henson et al., 2010). However, suitably long time series of phytoplankton data are restricted almost entirely to the Northeast Atlantic where they have been collected by the Continuous Plankton Recorder (Richardson et al., 2006). These studies find that the timing of the spring bloom has advanced by an average of 0.3 days per decade for some phytoplankton species from 1976 to 2005 (Edwards & Richardson, 2004).

The timing of the bloom is hypothesised to be important to the subsequent productivity of the marine ecosystem. The match-mismatch hypothesis (Cushing, 1990) states that changes in phytoplankton bloom timing may increase or decrease the survival of zooplankton and fish larvae. This effect has been demonstrated, for example, in observations of bloom initiation and haddock larvae in the northwest Atlantic (Platt, Fuentes-Yaco, & Frank, 2003), where earlier blooms led to increased survival of haddock larvae. The timing of shrimp hatching throughout the North Atlantic has also been shown to be coherent on interannual time scales with the timing of the phytoplankton bloom (Koeller et al., 2009). Phytoplankton phenology has also been hypothesised to affect the timing of oceanic CO_2 uptake in subpolar regions (Bennington, McKinley, Dutkiewicz, & Ulman, 2009; Palevsky & Quay, 2017), and seasonal variability in primary production alters the efficiency of carbon export and subsequent ocean storage (Lutz, Caldeira, Dunbar, & Behrenfeld, 2007). Changes to the timing of the phytoplankton bloom associated with climate warming are therefore expected to have impacts on the marine food web and carbon cycling.

Knowledge of contemporary interannual variability in phytoplankton phenology has principally originated from satellite ocean colour observations which provide the necessary temporal and spatial resolution to quantify the key features of the seasonal cycle. Despite a multitude of different approaches to determining the timing of bloom initiation (eg Brody, Lozier, & Dunne, 2013; Ji, Edwards, Mackas, Runge, & Thomas, 2010), there is general agreement on the large-scale patterns of phytoplankton phenology. The satellite-derived data demonstrate that the phytoplankton spring bloom starts ~ April in the subpolar North Atlantic, shifts to an autumn bloom (~ October) in the subtropics, and in the Southern Ocean starts ~ September (eg Cole, Henson, Martin, & Yool, 2012; Racault, Le Quere, Buitenhuis, Sathyendranath, & Platt, 2012). In addition, the timing of the spring bloom displays substantial interannual variability in response to meteorological and oceanographic conditions (Henson, Dunne, & Sarmiento, 2009; Taboada & Anadon, 2014). The phytoplankton seasonal cycle is expected to be altered by climate change, principally via increasing stratification in response to warming (Doney, 2006). This is expected to lead to earlier bloom timing in subpolar regions, as light limitation is alleviated earlier in the growing season (Henson, Cole, Beaulieu, & Yool, 2013). In the North Atlantic, a dramatic decrease in PP is predicted, associated with a transition from the current spring blooming regime to an autumn blooming regime by the end of the century (Henson et al., 2013), driven principally by increased stratification and the accompanying reduction in nutrient supply.

Analyses of future phytoplankton phenology have to date been restricted by the coarse temporal resolution (typically monthly) of climate model output. Monthly resolution data are known, however, to result in reduced accuracy and precision in bloom timing estimates in satellite data, compared to weekly or daily resolution data (Ferreira, Visser, MacKenzie, & Payne, 2014). In Henson et al. (2010), an analysis of modelled annual PP found that ~30–40 years of data would be needed to distinguish a climate change trend from the background natural variability. The authors suggested that other indicators, such as phenology, may allow trends to be more rapidly detected than in annual PP. However, Henson et al. (2013) found, using monthly mean model output, that climate change trends in the seasonal amplitude of PP was no more rapidly detectable, still requiring ~30–40 years of data. The monthly resolution of the model output was, however, assumed to be hampering characterisation of the seasonal cycle and to be too coarse to pinpoint the start of the bloom. Hence, the authors suggested that monthly data were not suited to robust assessment of climate change trends in bloom timing, and that higher temporal resolution data could allow more rapid detection of climate change trends.

Here, we analyse model output from a coupled climate run over the period 2006–2100 at a range of temporal resolutions, from 5 to 30 days, to determine how estimates of bloom timing and climate change trends are affected by sampling frequency. In addition, we assess how the temporal and spatial resolution of observations may affect the ability to detect future trends in phytoplankton bloom initiation.

2 | MATERIALS AND METHODS

2.1 | Model output

We use the MEDUSA-2.0 biogeochemical model (Yool, Popova, & Anderson, 2013) coupled to the NEMO ocean model. MEDUSA is a medium-complexity model which includes two phytoplankton and two zooplankton groups. Surface chlorophyll concentration is the sum of separate and dynamic diatom and non-diatom chlorophyll components. The model was run at ¼° (~19 km) horizontal resolution, with 75 vertical levels increasing in thickness from 1 m at the surface to 200 m at abyssal depths. The simulation used a 24 min time-step, and output was saved as means of 5, 10, 15, 20 and 30 days. The model was forced at the surface using output from a simulation of the HadGEM2-ES Earth System Model (Jones et al., 2011). The forcing simulation was run between 2006 and 2100 under Representative Concentration Pathway 8.5 (RCP8.5), the high emissions end-member of IPCC's AR5 scenarios (Riahi et al., 2011). A full description of the model formulation and validation against observations can be found in Yool et al. (2013), Yool, Popova, and Coward (2015).

2.2 | Bloom timing metric

To calculate the date of bloom initiation we use the approach of Hopkins, Henson, Painter, Tyrrell, and Poulton (2015), which eliminates the use of annual median chlorophyll concentration to define a

threshold value (as previously commonly used, eg, Siegel, Doney, & Yoder, 2002; Henson et al., 2009). Brody et al. (2013) found that using annual median chlorophyll as a threshold results in bloom initiation estimates that are sensitive to the duration of the bloom, so that long-lasting blooms appear to have later start dates. The use of an annual median chlorophyll threshold poses a particular problem for satellite-based estimates of bloom timing as data can be completely absent during the winter months (Ferreira, Hatun, Counillon, Payne, & Visser, 2015). Although this issue does not affect model output, which has no gaps, to enable comparison of modelled bloom timing with satellite-derived estimates we use an adaptation of the annual median approach proposed by Hopkins et al. (2015). For each calendar year we first identified the date of peak chlorophyll concentration and then concatenated the preceding and following 6 months. The bloom threshold was defined as the pre-peak minimum chlorophyll concentration plus 5% of the difference between the minimum and maximum concentrations. The global-scale patterns of bloom timing are not sensitive to the choice of threshold (tested between 1% and 20%; Hopkins, 2014), therefore to be consistent with previous work (eg Siegel et al., 2002), a value of 5% is also used here. The date of bloom initiation is then the first data point above the threshold occurring prior to peak concentration. A diagram illustrating the approach can be found in Figure 1 of Hopkins et al. (2015).

2.3 | Satellite data

For comparison with model results we calculate bloom timing from satellite-derived chlorophyll concentration data following the same methodology, applied to MODIS-Aqua data for the period July 2002–December 2015. Daily, 9 km chlorophyll concentration data were downloaded from http://oceancolor.gsfc.nasa.gov/ and then averaged into 5, 10, 15, 20 and 30 day resolution. The data were spatially interpolated onto the same ¼° grid as the model output. A comparison of the satellite-derived and modelled bloom start date for 2007–2015 calculated on 5-day resolution data is shown in Fig. S1. Generally, the modelled start date is later than the satellite-derived date if the bloom occurs in boreal spring, and earlier than the satellite-derived date if the bloom occurs in austral spring.

2.4 | Trend calculations

The linear trend in bloom start date was calculated using:

$$Y_t = \mu + \omega X_t + N_t \quad (1)$$

where Y_t is the time series of bloom start date, μ is a constant term (the intercept), X_t is the time in years, ω is the magnitude of the trend (the slope) and N_t is the residual, or unexplained part of the

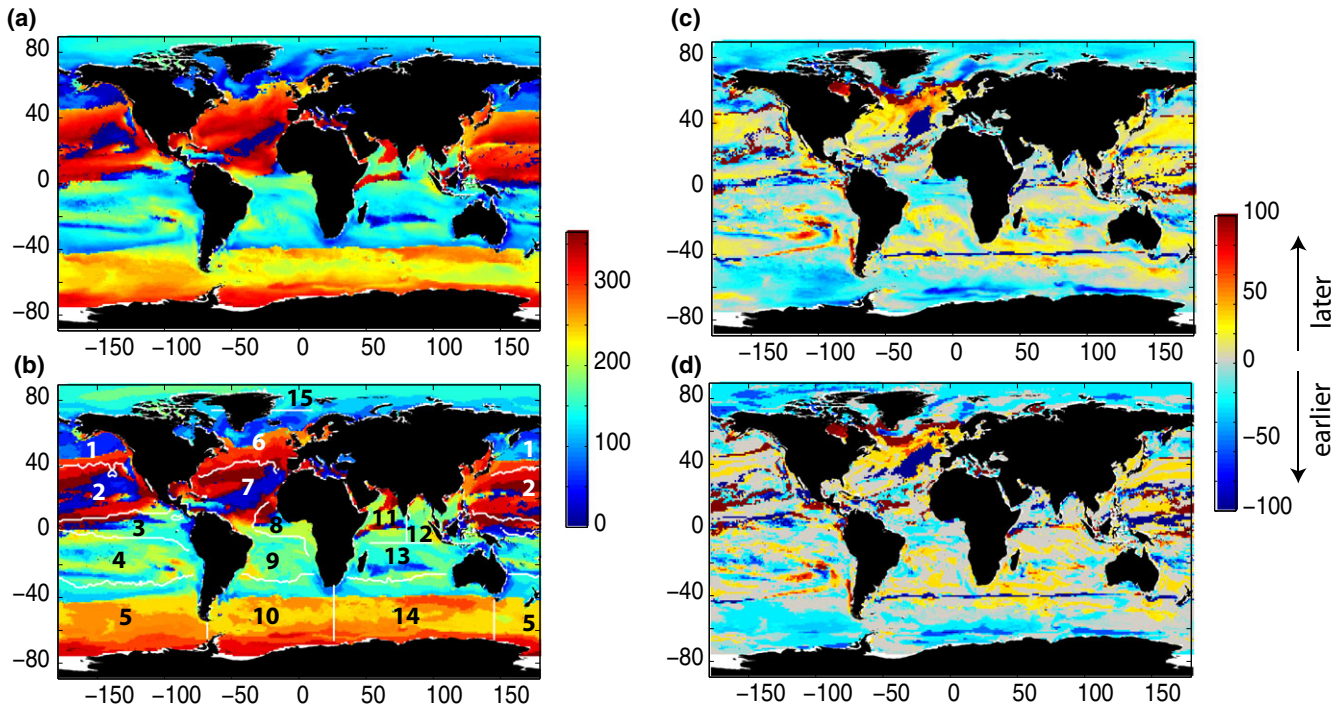

FIGURE 1 Median day of year of bloom initiation for years 2006–2025 in (a) 5 day resolution model output and (b) 30 day resolution output. Difference in day of year of bloom initiation by the end of the century (median of 2081–2100 minus median of 2006–2025) in (c) 5 day resolution model output and (d) 30 day resolution output. Biome boundaries are plotted in (b) and define: 1. High latitude North Pacific, 2. Oligotrophic North Pacific, 3. Equatorial Pacific, 4. Oligotrophic South Pacific, 5. Southern Ocean – Pacific sector, 6. High latitude North Atlantic, 7. Oligotrophic North Atlantic, 8. Equatorial Atlantic, 9. Oligotrophic South Atlantic, 10. Southern Ocean - Atlantic sector, 11. Arabian Sea, 12. Bay of Bengal, 13. Oligotrophic Indian Ocean, 14. Southern Ocean – Indian sector, and 15. Arctic Ocean [Colour figure can be viewed at wileyonlinelibrary.com]

time series. To prevent artefacts in trend estimates due to apparent discontinuities in the time series (ie a bloom starting on time-step 1 (starting 1st January) and a bloom starting on the last time step (ending 31st December) are only separated by 1 day, not 365 days), the cyclic nature of the calendar is accounted for, following Cole (2013).

The number of years of data needed to detect a trend against the background of natural variability is calculated following Tiao et al. (1990) and Weatherhead et al. (1998). To detect a trend with a probability of 90%, the number of years of data required (n^*), is:

$$n^* = \left[\frac{3.3\sigma_N}{|\omega|}\sqrt{\frac{1+\phi}{1-\phi}}\right]^{2/3} \quad (2)$$

where σ_N is the standard deviation of the noise (ie the residuals from the trend fitting), ω is the estimated trend and ϕ is the auto-correlation of the AR(1) noise represented by $\phi = \mathrm{Corr}(N_t, N_{t-1})$.

2.5 | Spatial averaging

To investigate the influence of temporal resolution on n^* on a basin scale, we use the biomes defined in Henson et al. (2010). The boundaries and names of the fourteen biomes are shown in Figure 1b. To assess the influence of spatial averaging on trend detection, we also compare n^* calculated at single locations with that calculated from data spatially averaged over a representative area. The locations selected are ocean observing stations that include a biogeochemical component (http://www.oceansites.org). The representative area (or 'footprint') of a station is considered to be the region that has a similar mean and variability (within ± 2 standard deviations) as the time series at the station itself (full methodological details can be found in Henson, Beaulieu, & Lampitt, 2016). Here, we calculate the footprint for each station using the monthly MEDUSA chlorophyll concentration. We refer to n^* calculated at a single station (ie single pixel) as 'spatially discrete' and n^* calculated over a footprint as 'spatially averaged'. To calculate spatially averaged n^*, the time series of bloom start dates is first averaged over the relevant footprint, and then the trend and thence n^* are calculated.

3 | RESULTS

3.1 | Effect of temporal resolution on bloom timing estimates

The median bloom start date (for 2006–2025) calculated on both the 5 day and 30 day resolution model output is shown in Figure 1a,b (results for all temporal resolutions are shown in Fig. S2). The global-scale patterns are broadly similar in the two resolutions. High latitude blooms begin in spring (March-April in the northern hemisphere and October-November in the southern hemisphere). In temperate and subtropical regions blooms start in autumn/winter (November-December in the northern hemisphere and July-August in the southern hemisphere). These large-scale patterns are similar to the satellite-derived estimates (Fig. S1), although the model tends to estimate spring bloom start dates that are ~50 days later than estimated from the satellite data. The model also estimates the southern hemisphere subtropical bloom start date to be ~50 days earlier than the satellite estimate. In both cases, the oligotrophic gyres are the regions which exhibit the greatest discrepancy between the satellite-derived and model-derived bloom timing estimates, possibly because oligotrophic gyres tend to have a relatively weak seasonal cycle in chlorophyll concentration and so satellite-derived estimates of bloom timing are somewhat ambiguous (eg Cole et al., 2012). Due to the potential errors in satellite-based bloom timing estimates in gyre regions, it is unclear whether the model-based estimates are robust. We therefore do not disregard the model-derived bloom timing estimates in these regions in our subsequent analyses.

Decreasing the temporal resolution of the model output does not alter the broad-scale patterns of bloom timing, but locally there are differences. Pixels where the average bloom timing is statistically similar (ANOVA, $p > .05$) in the 5 day and 30 day output comprise only 31% of pixels. In the majority of the ocean therefore, the temporal resolution of the time series does affect the estimated bloom start date. Almost universally (85% of pixels), 30 day resolution data results in later estimated bloom start date than the 5 day resolution output by, on average, 25 days. A probability density plot of the bloom start date for all temporal resolutions demonstrates that the 30 day resolution data also has a substantially different distribution from the 5 day data (Figure 2a), partly because the 30 day data is constrained to take one of only 12 values (ie 15th January, 15th February etc.). However, for temporal resolution up to 20 days, the distribution of start dates is very similar to the highest resolution data. A similar effect is seen in the satellite data (Fig. S1d), where 30 day resolution data results in bloom initiation estimates ~20 days later than in the 5 day resolution data.

3.2 | Climate change-driven trends in bloom timing

The change in bloom start date between the first 20 years (2006–2025) and the last 20 years (2080–2099) of the model run forced with the IPCC RCP8.5 scenario shows that bloom initiation is generally predicted to become later in the northern hemisphere subtropics (ie. shifting from a spring to an autumn start) and earlier in the tropics and the Southern Ocean (Figure 1c,d). Changes in bloom timing by the end of the century are typically of the order of ± 20 days, with larger shifts found at the leading edges of expanding subtropical gyres. The observed patterns are consistent with previous work that found a decrease in the seasonal amplitude of mixed layer depth and thus nutrient supply, which resulted in a transition of northern hemisphere subpolar regions (spring initiating blooms) to more subtropical-like conditions with later autumn blooms (Henson et al., 2013). In the subpolar north Atlantic, the changes in bloom timing are more pronounced than in the Pacific, and a larger region transitions to autumn bloom conditions. In the Southern Ocean and Arctic regions, earlier bloom initiation is prevalent, likely in response

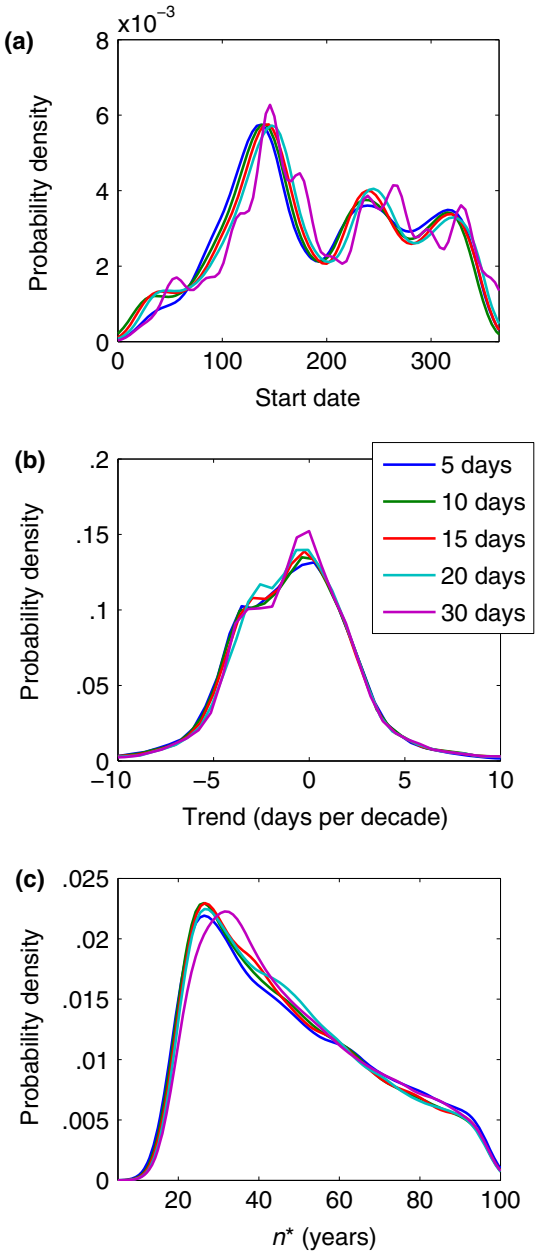

FIGURE 2 Probability density plots for global data on (a) median day of year of bloom initiation for years 2006–2025, (b) linear trend (days/decade) in bloom timing date from 2006 to 2100, and (c) n^* (years), the number of years of data needed to distinguish a trend in bloom timing from the background of natural variability. In each plot, the probability density distribution for 5, 10, 15, 20 and 30 day resolution model output is shown [Colour figure can be viewed at wileyonlinelibrary.com]

to earlier shoaling of the mixed layer and thus alleviation of light limitation. (Note however that the model does not include sea-ice algae, so cannot predict potential alterations in bloom timing in ice-covered regions). The low seasonality generally present in oligotrophic regions renders the analysis of phenology less relevant, and little change in bloom timing is observed, except at the edges of expanding gyres. The patterns of change in bloom timing at the broad-scale are similar in the 5 day and 30 day resolution data. Indeed, globally, the median change in bloom timing by the end of the century is essentially the same: 6 days earlier for 5 day resolution and 4.5 days earlier for 30 day resolution. Therefore, although the bloom initiation date itself depends on the temporal resolution of the data, the changes in timing induced in a global warming scenario are similar, regardless of temporal resolution.

The trend in bloom timing between 2006 and 2100 for both the 5 day and 30 day resolution model output is shown in Figure 3a,b (results for other temporal resolutions are shown in Fig. S3). Later bloom start dates are predicted in the future for the northern hemisphere subpolar regions and earlier for the Southern Ocean and Arctic. At 5 day resolution, trend magnitudes are on the order of 5–10 days later per decade in the subpolar northern hemisphere and 5–10 days earlier in the Arctic and Southern Ocean. At 30 day resolution, the trend magnitude is statistically different from the 5 day resolution in only 10% of the ocean (ANCOVA test, 95% significance level). The similarity in trends is confirmed in Figure 2b where the distribution of trends for all temporal resolutions are plotted. The coarser temporal resolution data is slightly more likely to result in a zero trend than the 5-day resolution data, but otherwise the predicted trend magnitude is very similar. The predicted trends in bloom timing under the IPCC's business-as-usual scenario are therefore almost identical irrespective of the temporal resolution of the data.

3.3 | Effect of temporal resolution on trend detection

The number of years of data required to distinguish a climate change trend from the background of natural variability, n^*, is shown in Figure 3c,d for 5 day and 30 day resolution (results for other temporal resolutions are shown in Fig. S4). Large regions of the low latitudes display trends that are undetectable before 2100. At high latitudes, 20–30 years of data are needed, increasing to >40 years in parts of the Arctic and high latitude North Atlantic. These values are consistent with previous studies that have shown that robustly detecting long-term trends in the seasonal amplitude of chlorophyll concentration or PP requires 30–40 years of data (Henson et al., 2013). The patterns of n^* are very similar in both the 5 day and 30 day resolution output and, as a global median, n^* is essentially identical (43.5 years for 5 day and 44 years for 30 day, with 32% of pixels showing trends that are undetectable before 2100 in both resolutions). This reflects the similarities in the magnitude of the trend calculated for the 5 day and 30 day resolution time series. The probability distribution plot for all temporal resolution data demonstrates that lower resolution data have almost no effect on n^* (Figure 2c), particularly if n^* is shorter than 20 years or longer than 50 years. The exception is the 30 day resolution data, in which the mode of n^* is 32 years, compared to 27 years for higher temporal resolutions. Generally, increasing the temporal resolution of the data therefore does not reduce the number of years of data needed to detect a climate change-driven trend in bloom timing.

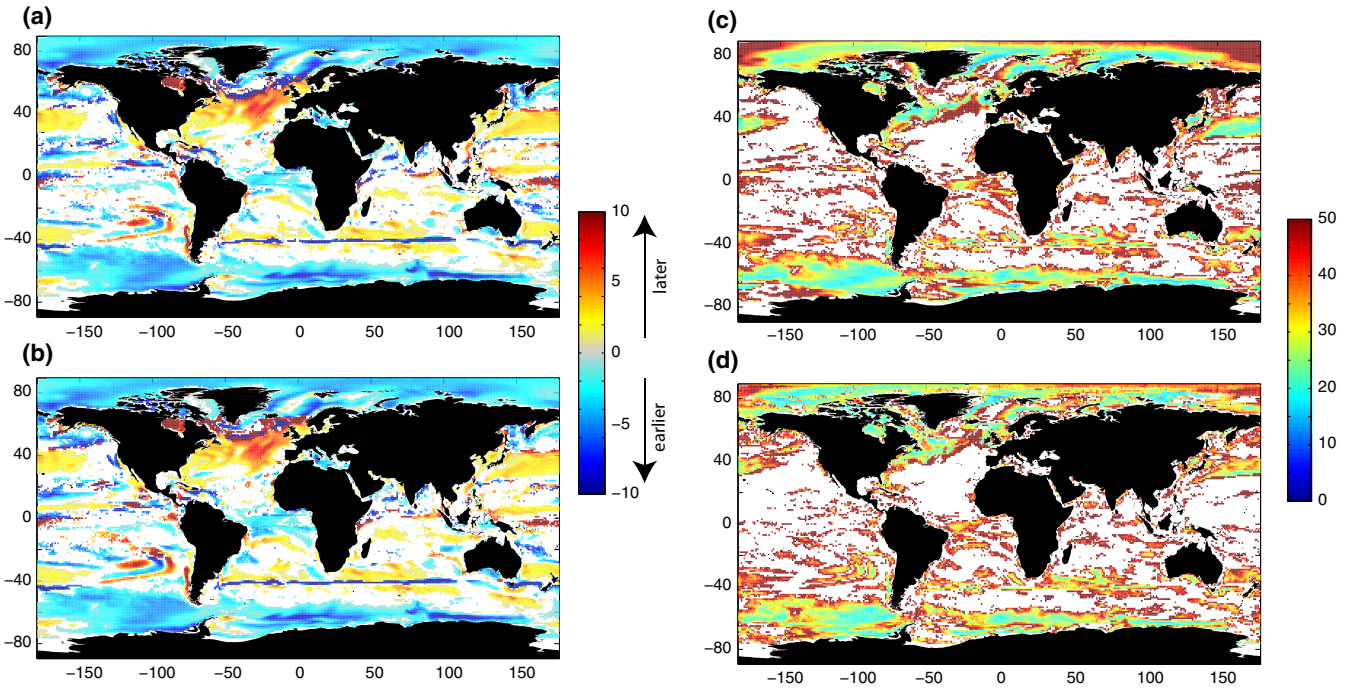

FIGURE 3 Linear trend (days/decade) in bloom timing for 2006–2100 calculated using (a) 5 day and (b) 30 day resolution model output. White areas correspond to areas with non-significant trends (95% confidence limit). Number of years of data needed to distinguish a long-term trend from the background natural variability, n^*, calculated using (c) 5 day and (d) 30 day resolution model output. White areas correspond to where n^* exceeds 100 years [Colour figure can be viewed at wileyonlinelibrary.com]

3.4 | Effect of spatial scale on trend detection

We investigate whether spatial averaging affects n^* at two scales: basin scale and regional scale. The biome average n^* for bloom initiation date is plotted in Figure 4 for all temporal resolutions. Probability density plots for all biomes and temporal resolutions can be found in Fig. S5. The biomes with the shortest n^* (5 day resolution data) are the Arctic (33 years), Southern Ocean Pacific sector (36 years) and the high latitude North Atlantic (39 years); those with the longest n^* are the Arabian Sea (67 years), Equatorial Pacific (64 years) and the North Atlantic oligotrophic gyre (64 years). In most cases at the basin scale, n^* changes relatively little with increasing temporal resolution; in others, n^* may increase or decrease as resolution varies, but there is no consistent pattern.

The influence of spatial averaging on the length of time series needed to detect a trend in bloom timing at the regional scale is illustrated in Figure 5. For each time series station (Figure 5a), n^* calculated at the pixel closest to the station ('spatially discrete') is compared to n^* calculated using footprint-mean start date ('spatially averaged'). All calculations were performed on the 5 day temporal resolution model output. For the majority of stations assessed, spatially averaging the data before n^* calculation decreases the length of data record needed to detect a trend (compare red and blue bars in Figure 5b). Of a total of 28 sites, 16 have reduced n^* with spatial averaging (of which, n^* is reduced to <100 years at 5 sites). At three sites, n^* is almost identical (±2 years) regardless of averaging, while at a further three sites n^* increases with spatial averaging. At six sites, n^* exceeds 100 years regardless of spatial averaging. As with the biome-scale data, there is no consistent increase or decrease in n^* with increasing temporal resolution (Fig. S6).

As n^* is a function of both the magnitude of the trend and of the noise, differences in either factor may alter n^*. By spatially averaging the bloom start dates prior to calculating n^*, the trend is amplified for ~ 50% of stations, but importantly the noise is substantially reduced for 75% of stations. Together, these factors reduce n^* so that a long-term trend is generally more rapidly detectable in spatially averaged, rather than spatially discrete, time series. Our results imply that spatially resolved data therefore provide the best chance of detecting a climate change-driven trend in bloom timing.

3.5 | Limitations

The analysis presented here is limited to a single biogeochemical model for which relatively high temporal resolution data were available. The projections of spatial patterns, changes and trends in bloom timing are likely to be model-dependent, and therefore our results should be applied with due prudence. For instance, models differ considerably in their ecological structure and parameterisation (eg Kwiatkowski et al., 2014). This will affect the degree to which their phytoplankton populations are regulated by nutrient availability or grazing control and thus their modelled patterns of phenology. Consequently, an immediate avenue for future work lies in evaluating the dependence of our results on the specific model used here.

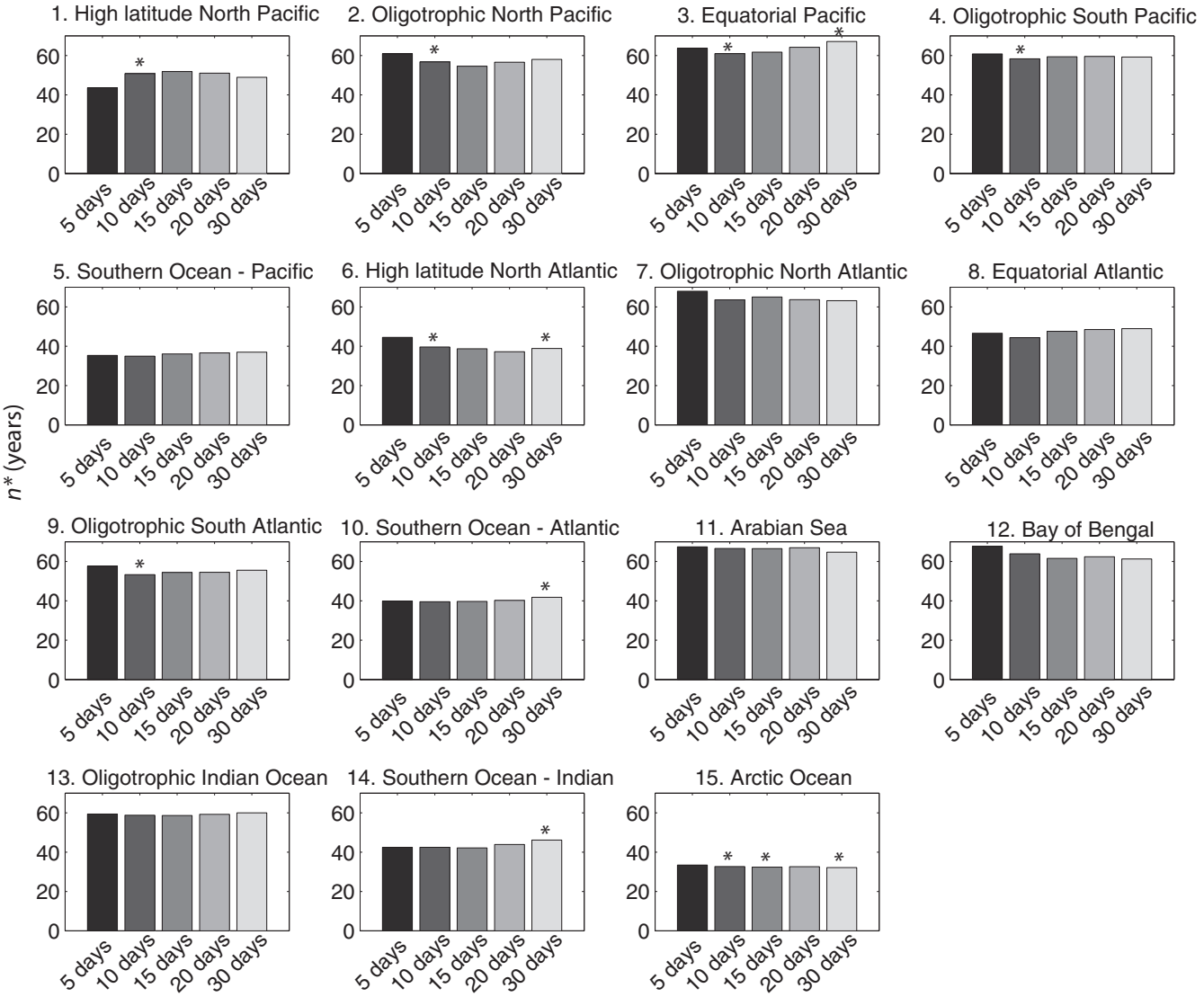

FIGURE 4 Biome median n^*, the number of years of data needed to distinguish a climate change-driven trend from natural variability, for model output at 5, 10, 15, 20 and 30 day resolutions. Biome boundaries are plotted in Figure 1b. An asterisk indicates that the biome mean n^* is different at the 95% level (ANOVA test) from the next highest resolution, eg, an asterisk above a 30 day resolution bar indicates that the mean n^* is significantly different from the 20 day resolution biome mean n^*

High temporal resolution surface chlorophyll output from several more global biogeochemical models will be available from 2018 through the CMIP6 process which will contribute to the IPCC AR6 report, at which point this analysis should be revisited to quantify the inter-model differences in phenology. In addition, a maximum temporal resolution of 5 days has been used here as the baseline against which results from coarser resolution output are assessed. However, even higher resolution data may give different results, although our analysis suggests this is unlikely (eg Figure 2). The maximum resolution practical for assessing phenology is likely to be daily; firstly, sub-daily data are rarely available and secondly, higher resolution data is likely to increase the magnitude of the noise without imparting additional phenological information.

The results presented here regarding the temporal resolution of data suitable for detecting trends in phytoplankton phenology may not apply to other variables or indicators of biological change. For example, previous work assessing annual integrated PP concluded that n^* was of a similar order of magnitude as found here for bloom timing (Henson et al., 2010). However, it may be that trends could be more rapidly detectable if seasonal information were retained in the analysis as it would increase the number of data points, although the auto-correlation associated with the seasonal cycle would have to be properly accounted for in the trend analysis. Alternative phenological metrics may also display more rapidly detectable trends, for example the duration of blooms or the timing of peak primary production.

Despite these limitations, this study provides a useful framework for considering the temporal and spatial data requirements necessary to characterise the timing of the phytoplankton bloom and its response to climate change.

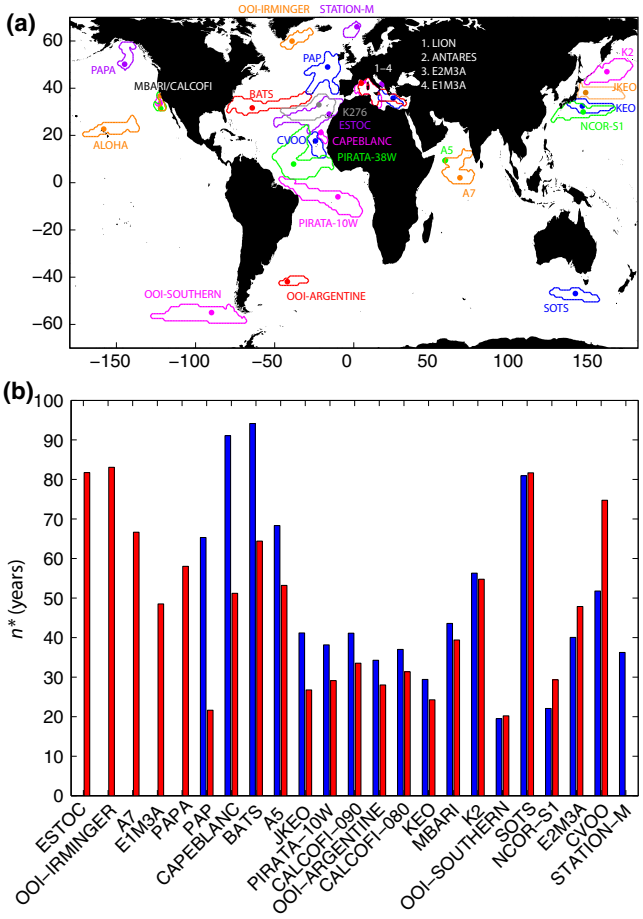

FIGURE 5 (a) Map of time series stations considered here and their spatial footprints in chlorophyll (see Methods). (b) Comparison of n^* for bloom start date calculated at biogeochemical time series stations (spatially discrete; blue bars) with n^* calculated over the relevant footprint (spatially averaged; red bars). Where bars are not plotted, n^* exceeds 100 years. If a station appears in (a) but not in (b), n^* remains greater than 100 years regardless of spatial averaging [Colour figure can be viewed at wileyonlinelibrary.com]

4 | DISCUSSION

4.1 | Predicted changes in phytoplankton phenology

Previous work on the future response of phytoplankton bloom phenology to climate change has been limited by the relatively coarse (monthly) temporal resolution of the available model output (Henson et al., 2013). Here, we use higher temporal resolution output to define the timing of bloom initiation from 2006 to 2100 and find significant trends in bloom timing under an IPCC 'business-as-usual' scenario. In the Arctic and high latitude Southern Ocean, the start of the spring bloom advances by ~5–10 days per decade, ie, by ~50–100 days by 2100 (Figure 3a,b). This is consistent with the suggestion that increasing stratification through warming and reduction in sea-ice leads to earlier alleviation of light limitation (eg Doney, 2006). This extends the length of the growing season and results in increased overall productivity of the polar regions (eg Bopp et al., 2013; Cabre, Marinov, & Leung, 2015). In the high latitude North Atlantic, bloom initiation shifts later by ~3–8 days per decade, ie, ~30–80 days by 2100 (Figure 1c,d) as a result of the expanding and intensifying oligotrophic gyres. Regions of the subpolar North Atlantic which currently experience high magnitude spring blooms are affected by shoaling winter mixed layers and subsequent reduction in nutrient supply (Henson et al., 2013). As these areas shift towards more subtropical-like conditions, phytoplankton phenology changes from a spring to an autumn initiating bloom. In the North Pacific, trends in bloom timing are weaker than at equivalent latitude in the North Atlantic, likely as a result of the less pronounced projected change in seasonal amplitude of the mixed layer depth (Henson et al., 2013). Tropical and oligotrophic regions have very weak, and often not statistically significant, trends in bloom timing (Figure 3a, b). Nutrient supply is already limiting to phytoplankton growth in these areas resulting in weak seasonality. Further warming, and hence stratification and reduced nutrient availability, in the climate change scenario acts to decrease the magnitude of phytoplankton blooms further (Henson et al., 2013), but does not change their phenology. The equatorial Atlantic is the only tropical region to show a coherent and statistically significant trend in bloom timing (Figure 3a,b). In this region, nitrate and dissolved iron supply is expected to increase slightly, potentially due to changes in wind-driven upwelling (Henson et al., 2013).

4.2 | Recommendations for observing changes in phytoplankton phenology

Although there is a general recognition that coarse temporal resolution data are likely to introduce errors into the estimation of bloom initiation, here we are able to quantify the effect. As temporal resolution decreases from 5 to 20 days, bloom timing generally shifts later by ~10 days although the probability distribution remains very similar (Figure 2a). An ANOVA test shows that in 69% of pixels, the bloom timing estimated from 30 day resolution output is statistically different (at the 95% level) from that calculated from the 5 day resolution data. This decreases to just 8% of pixels that have different bloom initiation estimates in 10 day resolution data compared to 5 day resolution data (29% for 15 day resolution, 48% different for 20 day resolution). Therefore, high temporal resolution data are required to determine the exact date on which the phytoplankton bloom starts.

As high temporal resolution data are needed to pinpoint bloom timing, is the same true for quantifying the climate change trend in bloom initiation? We find that an increase in temporal resolution does not substantially alter the magnitude or spatial pattern of the long-term trend in timing (Figure 3a,b and Fig. S3). At coarse temporal resolution, a larger proportion of pixels have a non-significant trend (at the 95% level), but otherwise the probability distribution of trends is very similar for all resolutions (Figure 2b). An ANCOVA test shows that in only 10% of pixels is the trend calculated from 30 day resolution output statistically different (at the 95% level)

from that calculated from the 5 day resolution data. This decreases slightly with increasing resolution: for 10 day resolution output, 2% of pixels have different trends compared to the 5 day data (3% for 15 day resolution, 4% different for 20 day resolution). The long-term trends in timing are therefore very similar, regardless of the temporal resolution of the data. This suggests that although the coarse temporal resolution data is not suitable for estimating the exact date of bloom initiation, the rate of change in bloom timing is adequately captured.

The similarity in the long-term trend in bloom initiation, regardless of temporal resolution of the data, results in similar values of n^*, the number of years needed to detect a climate change trend above the background of natural variability. For data with temporal resolution of 10–20 days, the distribution of n^* is very similar to that of the high resolution data (Figure 2). For the lowest resolution data (30 day), the distribution is similar to the high resolution data for small (<20 years) and large (>50 years) n^*, although the most frequently occurring n^* shifts from 27 to 32 years. Increasing the temporal resolution of the data therefore has little effect on the rapidity with which climate change-driven trends in bloom timing can be detected. Henson et al. (2013), using 30 day resolution data, found that the global average n^* for the seasonal amplitude (maximum minus minimum value for a given year) of PP was 36 years. They hypothesised that using higher resolution output would allow phytoplankton phenology to be more appropriately quantified and thus perhaps permit more rapid detection of long-term trends. However, we find that although bloom timing is indeed poorly estimated in low resolution data, this has little impact on the magnitude of trends in timing, and therefore the number of years of data needed to detect a climate change-driven trend.

We therefore provide the following recommendations for quantifying change in phytoplankton phenology. If defining the exact date on which the bloom starts is the priority, the highest temporal resolution data possible should be used. For example, if the aim is to link bloom timing in a particular year with a specific trigger, such as shoaling of the mixed layer. However, if the priority is determining the rate of change in bloom initiation, or detecting long-term trends in bloom timing, a temporal resolution of ~ 20 days is likely to be adequate. For example, if the aim is to assess the decadal anomalies in bloom timing in response to external forcing, eg, increasing ocean temperature.

4.3 | Implications for ocean observing systems

In addition to our results regarding the temporal resolution of data needed to detect trends in phytoplankton phenology, the spatial resolution should also be considered (Henson et al., 2016). Here, we compare estimates of n^* for spatially averaged and spatially discrete data (see Methods for definition of these terms) for selected time series stations. For the majority of stations, calculating n^* using spatially averaged data results in a reduction in n^* compared to using spatially discrete data (Figure 5b). Averaging the data prior to calculating the trend, and thence n^*, tends to amplify the magnitude of the trend and, importantly, also tends to reduce the noise term of the n^* calculation (Equation 2) so that the trend is more readily detectable. Note however that even with spatial averaging of the data, no consistent change in n^* with increasing temporal resolution is evident (Fig. S6).

If we wish to rapidly detect a climate change-driven trend in phytoplankton phenology, our results suggest that a data source capable of providing moderately high temporal resolution data (<20 days) and sufficient spatial coverage to allow for a degree of spatial averaging is needed. The ideal time series would also be sufficiently long to robustly characterise natural variability and be relatively insusceptible to discontinuities, which act to increase n^* (Beaulieu et al., 2013). Discontinuities might arise through gaps in the dataset or a change in instrument or sensor without the overlap needed to cross-calibrate with existing data.

The optimal dataset for studying trends in phytoplankton phenology is therefore ocean colour satellite-derived data. Consistent records are available since late 1997 (eg ESA OC-CCI data) and the data provide good coverage at 20 day resolution, which compensates for lack of data on individual days due to cloud cover (Cole et al., 2012). The data are spatially resolved so that averaging of data can be performed on multiple scales, and observations have thus far been sustained with no gaps and with sufficient overlap to allow for cross-calibration. The recent launch in February 2016 of the Ocean and Land Colour Instrument on ESA's Sentinel-3 satellite should ensure continued data on phytoplankton phenology until at least 2024 (planned mission lifetime). Maintaining a consistent satellite ocean colour record beyond Sentinel-3 will be critical to detecting climate change trends in phytoplankton, particularly as the time series begins to approach the length hypothesised to allow robust detection of long-term trends (~30 years; Henson et al., 2010, 2013).

An additional dataset with the potential to identify trends in bloom timing is the bio-Argo network (Claustre, 2011). This uses a globally distributed fleet of profiling floats to measure ocean properties, including chlorophyll fluorescence profiles. The profiles are typically obtained every 10 days, which meets our recommendation on temporal resolution (see previous section). However, spatial coverage by bio-Argo floats is not yet sufficiently dense in most ocean regions for spatial averaging to be a viable option. In addition, the data record is not yet long enough to distinguish climate change-driven trends from natural variability. Continued investment into the bio-Argo network, which ultimately aims to reach 1,000 floats (Johnson & Claustre, 2016), will ensure in situ, long-term monitoring of changing phytoplankton phenology, including of the expected changes in the vertical distribution of phytoplankton populations with ongoing climate change (eg Ishida et al., 2009; Lawrence, Popova, Yool, & Srokosz, 2015).

4.4 | Implications for marine ecosystems

In many regions, the predicted change in bloom initiation timing is substantial. The central tenet of the 'match-mismatch' hypothesis is

that higher trophic levels that rely on plankton as their principal food source may not be able to alter their phenology to match the interannual variability in bloom timing (Cushing, 1990). This may lead to food shortages if predator life stages which depend on the bloom occur too early or late relative to peak primary production. However, over longer than interannual timescales, phytoplankton grazers are expected to be able to adapt to changing conditions, including timing of food availability (eg Dam, 2013). Therefore, any changes in bloom timing which persist on multi-year timescales (eg long-term trends) may not have direct negative consequences on phytoplankton grazers. Timing of food availability is not the only consideration, however, as increasingly stratified (and nutrient limited) conditions are expected to alter the phytoplankton community structure. Shifts from diatom dominated to smaller phytoplankton dominated systems, as currently found in non-bloom forming regions, are predicted (Laufkotter, Vogt, & Gruber, 2013; Marinov, Doney, & Lima, 2010), which typically support less abundant higher trophic level populations. In addition, a reduction in total annual PP is also predicted for many regions due to increased nutrient limitation (with the exception of the polar oceans; Bopp et al., 2013; Cabre et al., 2015). In combination, the changes in phytoplankton phenology and overall productivity are likely to have subsequent negative impacts on the marine food web.

ACKNOWLEDGEMENTS

The modelling work was funded by NERC National Capability funding and the Regional Ocean Modelling project (ROAM; grant NE/H017372/1), as well as the FP7 EURO-BASIN project (grant agreement 264933). Model simulations used the ARCHER UK National Supercomputing Service (http://www.archer.ac.uk). Model output used here can be obtained from SAH on request. HSC and JH were supported by NERC PhD studentships.

ORCID

Stephanie A. Henson http://orcid.org/0000-0002-3875-6802
Jason Hopkins http://orcid.org/0000-0002-0454-4342
Andrew Yool http://orcid.org/0000-0002-9879-2776

REFERENCES

Beaulieu, C., Henson, S. A., Sarmiento, J. L., Dunne, J. P., Doney, S. C., Rykaczewski, R. R., & Bopp, L. (2013). Factors challenging our ability to detect long-term trends in ocean chlorophyll. *Biogeosciences*, *10*(4), 2711–2724.

Bennington, V., McKinley, G. A., Dutkiewicz, S., & Ulman, D. (2009). What does chlorophyll variability tell us about export and air-sea CO2 flux variability in the North Atlantic? *Global Biogeochemical Cycles*, *23*, GB3002. https://doi.org/10.1029/2008GB003241

Bopp, L., Resplandy, L., Orr, J. C., Doney, S. C., Dunne, J. P., Gehlen, M., … Vichi, M. (2013). Multiple stressors of ocean ecosystems in the 21st century: Projections with CMIP5 models. *Biogeosciences*, *10*(10), 6225–6245.

Brody, S. R., Lozier, M. S., & Dunne, J. P. (2013). A comparison of methods to determine phytoplankton bloom initiation. *Journal of Geophysical Research-Oceans*, *118*(5), 2345–2357.

Cabre, A., Marinov, I., & Leung, S. (2015). Consistent global responses of marine ecosystems to future climate change across the IPCC AR5 earth system models. *Climate Dynamics*, *45*(5–6), 1253–1280.

Claustre, H. (2011). Bio-Optical Sensors on Argo Floats. Reports of the International Ocean-Colour Coordinating Group, No. 11, IOCCG, Dartmouth, Canada.

Cole, H. (2013). The natural variability and climate change response in phytoplankton phenology, PhD Thesis, University of Southampton. Retrieved from http://eprints.soton.ac.uk/id/eprint/362006

Cole, H., Henson, S., Martin, A., & Yool, A. (2012). Mind the gap: The impact of missing data on the calculation of phytoplankton phenology metrics. *Journal of Geophysical Research-Oceans*, *117*, C08030. https://doi.org/10.1029/2012JC008249

Cushing, D. H. (1990). Plankton production and year-class strength in fish populations - an update of the match mismatch hypothesis. *Advances in Marine Biology*, *26*, 249–293.

Dam, H. G. (2013). Evolutionary adaptation of marine zooplankton to global change. *Annual Reviews of Marine Science*, *5*, 349–370.

Doney, S. C. (2006). Oceanography - Plankton in a warmer world. *Nature*, *444*(7120), 695–696.

Edwards, M., & Richardson, A. J. (2004). Impact of climate change on marine pelagic phenology and trophic mismatch. *Nature*, *430*(7002), 881–884.

Ferreira, A. S. A., Hatun, H., Counillon, F., Payne, M. R., & Visser, A. W. (2015). Synoptic-scale analysis of mechanisms driving surface chlorophyll dynamics in the North Atlantic. *Biogeosciences*, *12*(11), 3641–3653.

Ferreira, A. S., Visser, A. W., MacKenzie, B. R., & Payne, M. R. (2014). Accuracy and precision in the calculation of phenology metrics. *Journal of Geophysical Research-Oceans*, *119*(12), 8438–8453.

Gran, H. H., & Braarud, T. (1935). A quantitative study of the phytoplankton in the Bay of Fundy and the Gulf of Maine (including observations on hydrography, chemistry and turbidity). *Journal of the Biological Board of Canada*, *1*, 279–467. https://doi.org/10.1139/f35-012

Henson, S. A., Beaulieu, C., & Lampitt, R. (2016). Observing climate change trends in ocean biogeochemistry: When and where. *Global Change Biology*, *22*(4), 1561–1571.

Henson, S., Cole, H., Beaulieu, C., & Yool, A. (2013). The impact of global warming on seasonality of ocean primary production. *Biogeosciences*, *10*(6), 4357–4369.

Henson, S. A., Dunne, J. P., & Sarmiento, J. L. (2009). Decadal variability in North Atlantic phytoplankton blooms. *Journal of Geophysical Research-Oceans*, *114*, C04013. https://doi.org/10.1029/2008JC005139

Henson, S. A., Sarmiento, J. L., Dunne, J. P., Bopp, L., Lima, I., Doney, S. C., … Beaulieu, C. (2010). Detection of anthropogenic climate change in satellite records of ocean chlorophyll and productivity. *Biogeosciences*, *7*(2), 621–640.

Hopkins, J. (2014). A satellite perspective on global blooms of coccolithophores, PhD Thesis, University of Southampton. Retrieved from https://eprints.soton.ac.uk/374825/

Hopkins, J., Henson, S. A., Painter, S. C., Tyrrell, T., & Poulton, A. J. (2015). Phenological characteristics of global coccolithophore blooms. *Global Biogeochemical Cycles*, *29*(2), 239–253.

Ishida, H., Watanabe, Y. W., Ishizaka, J., Nakano, T., Nagai, N., Watanabe, Y., … Magi, M. (2009). Possibility of recent changes in vertical distribution and size composition of chlorophyll-a in the western North Pacific region. *Journal of Oceanography*, *65*(2), 179–186.

Ji, R. B., Edwards, M., Mackas, D. L., Runge, J. A., & Thomas, A. C. (2010). Marine plankton phenology and life history in a changing climate: Current research and future directions. *Journal of Plankton Research*, *32*(10), 1355–1368.

Johnson, K., & Claustre, H. (2016). Biogeochemical-Argo Planning Group. The scientific rationale, design and implementation plan for a biogeochemical-Argo float array.

Jones, C. D., Hughes, J. K., Bellouin, N., Hardiman, S. C., Jones, G. S., Knight, J., ... Zerroukat, M. (2011). The HadGEM2-ES implementation of CMIP5 centennial simulations. *Geoscientific Model Development*, *4*(3), 543–570.

Koeller, P., Fuentes-Yaco, C., Platt, T., Sathyendranath, S., Richards, A., Ouellet, P., ... Aschan, M. (2009). Basin-scale coherence in phenology of shrimps and phytoplankton in the North Atlantic Ocean. *Science*, *324*(5928), 791–793.

Kwiatkowski, L., Yool, A., Allen, J. I., Anderson, T. R., Barciela, R., Buitenhuis, E. T., ... Cox, P. M. (2014). iMarNet: An ocean biogeochemistry model intercomparison project within a common physical ocean modelling framework. *Biogeosciences*, *11*(24), 7291–7304.

Laufkotter, C., Vogt, M., & Gruber, N. (2013). Long-term trends in ocean plankton production and particle export between 1960-2006. *Biogeosciences*, *10*(11), 7373–7393.

Lawrence, J., Popova, E., Yool, A., & Srokosz, M. (2015). On the vertical phytoplankton response to an ice-free Arctic Ocean. *Journal of Geophysical Research: Oceans*, *120*(12), 8571–8582.

Lutz, M. J., Caldeira, K., Dunbar, R. B., & Behrenfeld, M. J. (2007). Seasonal rhythms of net primary production and particulate organic carbon flux to depth describe the efficiency of biological pump in the global ocean. *Journal of Geophysical Research-Oceans*, *112*, C1011. https://doi.org/10.1029/2006JC003706

Marinov, I., Doney, S. C., & Lima, I. D. (2010). Response of ocean phytoplankton community structure to climate change over the 21st century: Partitioning the effects of nutrients, temperature and light. *Biogeosciences*, *7*(12), 3941–3959.

Palevsky, H. I., & Quay, P. D. (2017). Influence of biological carbon export on ocean carbon uptake over the annual cycle across the North Pacific Ocean. *Global Biogeochemical Cycles*, *31*, 81–95. https://doi.org/10.1002/2016GB005527

Platt, T., Fuentes-Yaco, C., & Frank, K. T. (2003). Spring algal bloom and larval fish survival. *Nature*, *423*(6938), 398–399.

Poloczanska, E., Burrows, M., Brown, C., Garcia-Molinos, J., Halpern, B., Hoegh-Guldberg, O., ... Sydeman, W. (2016). Responses of marine organisms to climate change across oceans. *Frontiers in Marine Science*, *3*(62). https://doi.org/10.3389/fmars.2016.00062

Racault, M. F., Le Quere, C., Buitenhuis, E., Sathyendranath, S., & Platt, T. (2012). Phytoplankton phenology in the global ocean. *Ecological Indicators*, *14*(1), 152–163.

Riahi, K., Rao, S., Krey, V., Cho, C. H., Chirkov, V., Fischer, G., ... Rafaj, P. (2011). RCP 8.5-A scenario of comparatively high greenhouse gas emissions. *Climatic Change*, *109*(1–2), 33–57.

Richardson, A. J., Walne, A. W., John, A. W. G., Jonas, T. D., Lindley, J. A., Sims, D. W., ... Witt, M. (2006). Using continuous plankton recorder data. *Progress in Oceanography*, *68*(1), 27–74.

Rosenzweig, C., Casassa, G., Karoly, D. J., Imeson, A., Liu, C., Menzel, A., ... Tryjanowski, P. (2007). Assessment of observed changes and responses in natural and managed systems. In M. L. Parry, O. F. Canziani, J. P. Palutikof, P. J. van der Linden, & C. E. Hanson (Eds.), *Climate Change 2007: Impacts, adaptation and vulnerability. Contribution of Working Group II to the fourth assessment report of the intergovernmental panel on climate change* (pp. 79–131). Cambridge, UK: Cambridge University Press.

Siegel, D. A., Doney, S. C., & Yoder, J. A. (2002). The North Atlantic spring phytoplankton bloom and Sverdrup's critical depth hypothesis. *Science*, *296*(5568), 730–733.

Taboada, F. G., & Anadon, R. (2014). Seasonality of North Atlantic phytoplankton from space: Impact of environmental forcing on a changing phenology (1998-2012). *Global Change Biology*, *20*(3), 698–712.

Tiao, G. C., Reinsel, G. C., Xu, D. M., Pedrick, J. H., Zhu, X. D., Miller, A. J., ... Wuebbles, D. J. (1990). Effects of autocorrelation and temporal sampling schemes on estimates of trend and spatial correlation. *Journal of Geophysical Research-Atmospheres*, *95*(D12), 20507–20517.

Weatherhead, E. C., Reinsel, G. C., Tiao, G. C., Meng, X. -L., Choi, D., Cheang, W. -K., ... Frederick, J. E. (1998). Factors affecting the detection of trends: Statistical considerations and applications to environmental data. *Journal of Geophysical Research-Atmospheres*, *103*(D14), 17149–17161.

Yool, A., Popova, E. E., & Anderson, T. R. (2013). MEDUSA-2.0: An intermediate complexity biogeochemical model of the marine carbon cycle for climate change and ocean acidification studies. *Geoscientific Model Development*, *6*(5), 1767–1811.

Yool, A., Popova, E. E., & Coward, A. C. (2015). Future change in ocean productivity: Is the Arctic the new Atlantic? *Journal of Geophysical Research: Oceans*, *120*(12), 7771–7790.

SUPPORTING INFORMATION

Additional Supporting Information may be found online in the supporting information tab for this article.

How to cite this article: Henson SA, Cole HS, Hopkins J, Martin AP, Yool A. Detection of climate change-driven trends in phytoplankton phenology. *Glob Change Biol*. 2018;24:e101–e111. https://doi.org/10.1111/gcb.13886